1. Introduction

Winter flooding (WF) of harvested rice fields is an environmentally friendly agricultural practice, practiced especially in the USA, as an alternative to the burning of straw residues, which has a strong impact on air quality. In the USA, where burning straw is prohibited, more than 40% of rice fields are flooded during wintertime (Miller et al., 2010). Recently, this practice has been adopted also in a few geographical areas in southern Europe, such as southern France and northern Italy. Winter flooding consists in flooding rice fields during wintertime until early spring. Agronomic, environmental, hydrologic and economic reasons can push farmers to adopt this practice, which can be considered an excellent example of how agriculture can be compatible with the environment. Several authors reported agronomic benefits of winter flooding of rice fields, which include: (1) increasing straw decomposition rate; (2) inhibiting weed seed germination and postponing their winter growth (Fogliatto et al., 2010); (3) limiting erosion possibly due to ponding water protecting the soil (Brogi et al., 2015); (4) retaining sediments and nutrients thus improving the quality of runoff water, especially if rice fields are not tilled after harvesting (Manley, 1999); (5) leaching salts and other potentially detrimental substances from the root zone to deeper soil layers, thus reducing plant stress and increasing yields (Bachand et al., 2014); and (6) decreasing the straw mass thus possibly reducing tillage requirements in the following agricultural season (Anders et al., 2008). Thanks to such agronomic benefits, winter field flooding may limit land operation costs in the next spring, allowing rice to be planted into minimal straw residue (Koger et al., 2013) hence providing a direct economic benefit to farmers (Taghavi et al., 2015). Studies conducted in the south of France (Camargue) to estimate potential cost savings with respect to spring-field preparation for farmers who applied winter flooding, showed that this practice can be economically sustainable for farmers and most beneficial for society, providing various ecosystem services (Niang et al., 2016). In fact, in this study, the Authors showed that all the analysed scenarios adopting winter flooding performed better than no-winter flooding scenarios, with the best performance obtained by the ‘harvesting in flooded fields’ scenario. Total benefits to the farmer

were found to be 830 €/ha (about 904 $), total costs 193 €/ha (210 $), with a benefit to cost ratio of 4.3; moreover, total benefits to society were assessed to be 1752 €/ha (1909 $), total costs 258 €/ha (281 $), with a benefit to cost ratio of 6.8. Other possible benefits of winter flooding may include: (1) groundwater recharge to counteract the decrease in groundwater levels in areas in which this resource is strongly exploited for civil uses (e.g. drinking water supply) (Natuhara, 2013) or reduced as a consequence of severe dry periods (Taghavi et al., 2015); (2) flood risk reduction, if agricultural fields (including rice paddies) are used as flooding areas to decrease the pressure of floods on urban centres during late fall, winter and early spring storms (Taghavi et al., 2015); (3) reduction of pumping depth due to the increased groundwater level, thus reducing energy costs for different water uses; (4) improvement of groundwater quality as a result of the dilution effect of potentially problematic substances (salts, nutrients, etc.) due to the huge groundwater recharge provided in the case of extended flooded areas (Bachand et al., 2014). Nevertheless, with respect to this last point, other Authors reported that salts could increase locally in aquifers as a consequence of a concentration effect if areas are affected by salinity problems (Taghavi et al., 2015); lastly (5) supply of various ecosystem services, the main and the best known of which is the provision of extensive foraging habitats to wintering waterfowl and other wildlife (Brogi et al., 2015; Kaneko and Nakamura, 2011; Koger et al., 2013; Manley, 1999; Niang et al., 2016).

In many geographical areas, even not cultivated with rice, the artificial submersion of agricultural areas, often called Ag-MAR (where Ag stands for Agricultural and MAR for Managed Aquifer Recharge) is used to overcome two major hydrological issues related to the climate change: severe and chronic groundwater overdraft in the summer season, and flood risks from winter storms. Ag-MAR is usually carried out during the winter, when water is abundant since it is not used for irrigation and can therefore be used to recharge the groundwater reservoir (Niswonger et al., 2017). Recent research suggests that groundwater overdraft and flood risk can be mitigated by diverting flood waters onto agricultural lands both to meet crop consumptive demand and for direct groundwater recharge (Bachand et al., 2016, 2014). Ag-MAR has been recently adopted in a few

areas of the USA, particularly in California. Possible benefits of Ag-MAR with respect to groundwater recharge include: (1) structures for harvesting water already provided by the existent conveyance canals and irrigation systems (Niswonger et al., 2017); (2) achievement of recharge over large agricultural areas due to the connection of rivers with the irrigation channel network, which can convey water to fields even very far from each other, as compared to more localized methods of recharge such as injection; (3) absence of competition for land use, since agricultural land would be otherwise fallow in most cases; (4) extremely low evaporation losses, due to the low winter temperatures: more than 90% of water applied on the fields during winter submersion was shown to reach the surface aquifer in California (Dahlke et al., 2018). Some Authors reported that winter flooding may improve the availability of soil moisture in early spring (Taghavi et al., 2015), which could be useful for crop production. Despite this, Mayer et al. (2019) simulated different irrigation management scenarios through a surface water-groundwater modelling tool applied to an irrigation district of 1000 ha in northern Italy, and highlighted that the winter flooding of rice fields adopted in the district was carried out too early in the season (from November 15th to January 15th) to be able to influence soil moisture and groundwater levels at the beginning of the agricultural season (end of April-beginning of May). The Authors hypothesized that winter flooding needs to be more prolonged in order to maintain a higher water table at the beginning of summer, which would allow to increase the irrigation efficiency of rice during the cropping season.

Niswonger et al. (2017), developed a methodology for the simulation of MAR on a 700 km^2 area, using the distributed groundwater flow model MODFLOW on a 24 years period, including 7 years of winter flooding. Results showed that in the 7 years in which Ag-MAR was applied, the annual groundwater recharge increased of 9-12%. Kennedy (2015) found that the groundwater recharge during wintertime was four times greater than that associated with the harvest flooding for cranberries. Additionally, the same study showed how the groundwater recharge from winter flooding might constitute a short time and small spatial scale benefit, since the hydrologic response of wells far from the flooded sites was very weak. In fact, groundwater was shown to be recharged

only very close to the flooded areas, whereas groundwater levels measured in wells located 100 meters or more from them were not affected by the practice. According to the Author, the area of influence around a flooded surface may vary seasonally in response to antecedent soil moisture and pre-flood groundwater elevation, as well as to soil characteristics, farm drainage infrastructures, and flooding holding time (Kennedy, 2015). Chen et al. (2002) illustrated in their paper the results of a series of numerical simulations conducted through the SAWAH model (one dimensional and Darcy-based; Wopereis et al., 1994), while the FEMWATER model (three dimensional, physically based; Lin et al., 1997) was used to differentiate lateral seepage from vertical percolation deriving from surface infiltration. This method allowed the computation of the ratio lateral seepage/vertical infiltration, and therefore the evaluation of the deep percolation (equal to the effective groundwater recharge). Since in the study area concrete bunds replaced earth ones to ease maintenance, the simulation did not account for lateral seepage through bunds of paddies ~~(Chen et al., 2002)~~, but only for horizontal water movement~~s~~ in the unsaturated zone under the bunds due to matric potential gradients ~~in the matric potential~~. The study concluded that the major lateral seepage flux for a paddy field occurs along the boundary of dry land/flooded paddy. In particular, the study shows that the surface infiltration flux is split into lateral seepage and groundwater recharge fluxes, which represent 24% and 76% of the total surface infiltration flux in the case of a 48 ha paddy field with a groundwater table at a 10 m below the soil surface. These percentages are not constant, but they are dependent on the spatial dimension of the flooded area (lateral seepage fluxes are larger in the case of smaller flooded surfaces). For an irrigation unit of 12 ha (i.e. total flooded area reduced by 75%) the two fluxes become 29% and 71% of the total infiltration. Even if not explicitly stated in the paper, the rate of groundwater recharge over surface infiltration is expected to increase for a shallower water table, approaching 100% when the water table reaches the soil surface.

The implementation of winter flooding of rice paddies was included in the Rural Development Program of the European Union, bringing economic benefits to farmers who practice it (Serra et al., 2007). The implementation of such practice varied considerably among paddy areas (from 0.17% of

the total rice surface in the Vercelli province in Italy, to 62% in the Ebro Delta and Albufera de Valencia in Spain), due to local differences in environmental policies application in the years 2002-2012 (Pernollet et al., 2015). In Italy, the practice of winter flooding of rice areas is still not widespread (about 3-4% in the winter 2019-20), probably because little information on the advantages and drawbacks of this practice is available and, contemporaneously, the winter irrigation supply has not been granted in all rice areas by the irrigation management agencies. If information concerning the agronomic advantages and disadvantages of this technique in rice areas is scarcely available, even fewer studies have dealt with the effects of winter flooding on the water resources cycle (soil water balance, groundwater recharge and levels). The RISTEC project (EU-RDP 2017) represents a first attempt to conduct a multidisciplinary study on winter flooding in the main Italian rice basin, located across the border between Lombardy and Piedmont regions in northern Italy. It started in October 2017 in three experimental sites cropped with rice during summertime. In this paper, the effects of winter flooding on groundwater levels and on the terms of the soil water balance for the three experimental sites are illustrated and discussed.

2. Materials and Methods

2.1 Study area

The three study areas were located about 50 km south east of Milan, in the Pavia province (PV), in the centre of the main Italian rice production area (Figure 1 - Box A). Their surface area ranged from 1.2 ha to 85 ha (Table 1), and they were surrounded by fallow fields during wintertime and by rice paddies in summertime.

In the E site (Figure 1 - Box E), characterized by six parcels of about 0.2 ha (20 x 80 m), different aspects of winter flooding were investigated, including nutrient cycling, agronomic benefits and GHGs emissions, together with hydrological effects. For this reason, only three parcels out six were subject to winter flooding (WF versus Dry in Figure 1), while during summer, wet seeding and

continuous flooding was applied to all six parcels. Since hydrological aspects are more easily quantifiable over larger areas, two wider pilot areas were taken into account (Z and C sites, Figure 1, boxes C and D respectively). In the Z site, the winter flooding practice was introduced in 2004 in the southern fields and gradually extended to the entire farm area in the successive years (the last fields were winter flooded for the first time in 2016). In the site, winter flooding is usually applied from October to the end of January-half of February, as water supply is abundant, and the farmer has a water right for diverting irrigation water from a channel independently from the irrigation authority, as far as a maximum limit is not exceeded. Conversely, in the C and E sites, winter flooding was first adopted in the fall of the 2016, as a consequence of the subsidy given to farmers by the EU-RDP, which, in the Lombardy Region, prescribes that at least 5 cm of water are applied for at least 60 consecutive days from harvest (September) to early spring (February). In the two sites winter flooding was applied approximatively between mid-November and mid-January, since this is the period in which the irrigation service was provided by the irrigation authority (Associazione Irrigua Est Sesia – AIES) managing irrigation water in the territory where the two pilot areas are located.

In this study, regular measurements were carried out in the three areas for two winters (2017-2018 and 2018-2019), while in the summer 2018 only the Z and E sites were monitored. During the summer, all the six parcels at the E site were managed following the water seeding and traditional flooding technique, and the Selenio rice variety was seeded. With respect to the Z site, the summer management was as follows: for four out of nine paddies included in the area (13.5 ha) the irrigation management was the same as for the E site, and the Carnaroli variety was seeded; for the remaining five fields (22.5 ha), a dry-seeding and delayed flooding technique was adopted, and the Sole CL and Selenio varieties were grown. Duration of winter and summer flooding in the study period are reported in Table 1.

Table 1

Site	Name	Size (ha)	Average elevation (m a.s.l.)	First year of WF application	Winter flooding periods	Summer flooding periods
E	Ente Nazionale Risi	1.2	107.70 ± 0.02	2016	from 16-Nov-17 to 06-Mar-18 (110 days); from 5-Nov-18 to 28-Feb-19 (115 days)	from 18-May-18 to 31-Aug-18 (105 days)
Z	Zanaglia	36	104.65 ± 0.64	2004	from 11-Oct-17 to 25-Jan-18 (106 days); from 14-Oct-18 to 24-Jan-19 (102 days)	from 17-Apr-18 to 10-Aug-18 (130 days, 90 of which had contemporaneous flooding of all the fields)
C	Capitolo	85	102.78 ± 0.44	2016	from 15-Nov-17 to 16-Jan-18 (62 days); from 15-Nov-18 to 12-Feb (89 days, 65 of which had contemporaneous flooding of all the fields)	-

2.2 Data collection and elaboration

The computation of the water balance for the three areas required the collection and elaboration of time series data and environmental information. Hourly time series of agro-meteorological variables (temperature, wind speed, relative humidity, precipitation and solar radiation) were collected for the period 2017-2019 at a station installed in the same farm as the E site (Castello D'Agogna, PV; meteo data source: Regional Environmental Protection Agency, ARPA), at about 5-7 km north from sites Z and C (Figure 1). Irrigation water flows entering and exiting the three pilot areas were measured using different devices and sensors, namely rectangular or trapezoidal-throated flumes linked to stilling wells equipped with pressure transducers connected to data-loggers. An acoustic-Doppler area-velocity flow meter (SonTek-IQ Standard, Switzerland) was used, instead of the flume, at the inlet section of the Z site. Flumes at the E site were dimensioned to fit the maximum discharge of 80 l s^{-1}, while irrigation inflow and outflow flumes at the C site fitted a maximum discharge of 500 l s^{-1} each. Finally, the outflow of the Z site was instrumented with two flumes designed to fit a maximum discharge of 120 l s^{-1} each. Rating curves were estimated using the WinFlume software (U.S.B.R., USA), as illustrated by Chiaradia et al. (2015). During the measuring period, water levels and discharge measurements were taken manually to adjust the

theoretical flow rate curves for in open field conditions. Groundwater levels were monitored within a total of 16 piezometers located inside and outside the winter flooded areas. Piezometric wells were made by PVC pipes (from 3 to 6 m long, 1.5 m windowed in the lower part) installed into holes drilled with a hand auger. In most wells, measurements were acquired continuously with pressure transducers connected to data-loggers, while in a few wells a manual water level meter was used to acquire data in periodical campaigns. Periodically, manual measurements were taken also in the instrumented wells. Lastly, a topographical survey of the three pilot areas, also assessing the position of the instrumentation, was performed through a differential GPS (site Z and C) and a Total Station (site E). Table 2 summarizes the equipment used in this study for data collection.

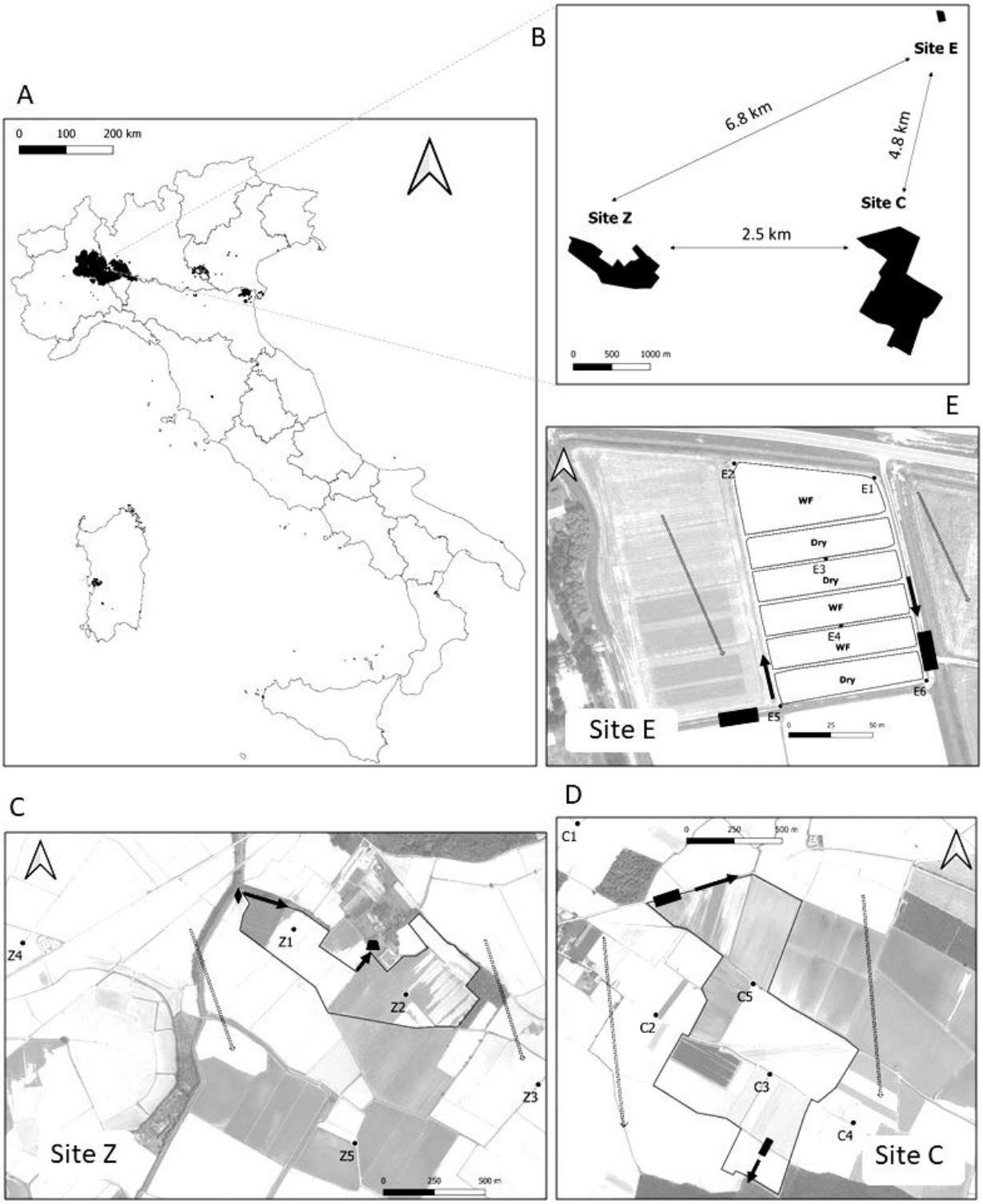

182

183 *Figure 1*

184

Table 2

Site	Type of variable	Meter	Characteristic dimensions (m)	Type of measure and recording system	Measuring range	Expected measurement error	Quantity	Notes
E	Water inflow	Rectangular-shaped long throated flume	0.3 large x 0.3 long (control section)	a	3-80 l s^{-1}	10 - 3%	1	(1)
E	Water outflow	Rectangular-shaped long throated flume	0.3 large x 0.3 long (control section)	a	3-80 l s^{-1}	10 - 3%	1	(1)
E	Groundwater level	Piezometer	0.04 diameter of the plastic tube; windowed part 1.5 long	a, b	0 - 5 m	± 0.01 m	6	(2)
Z	Water inflow	Area-velocity flow meter	1.0 large (measurement section)	d	± 1000 l s^{-1}	<10%	1	(3)
Z	Water outflow	Trapezoidal-throated flume	1.0 x 0.4 (control section) wall slope 45°	a	5-120 l s^{-1}	10 - 3 %	2	(1)
Z	Groundwater level	Piezometer	0.0381 diameter of the plastic tube; windowed part 1.5 long	b, c	0 - 5 m	± 0.01 m	5	(2)
C	Water inflow	Rectangular-shaped, with movable weir	movable crest weir: 1.0 large, 0.6 long	b	40-500 l s^{-1}	10 - 3 %	1	(1)
C	Water outflow	Rectangular-shaped, with movable weir	movable crest weir: 1.0 large, 0.6 long	b	40-500 l s^{-1}	10 - 3 %	1	(1)
C	Groundwater level	Piezometer	0.0381 diameter of the plastic tube; windowed part 1.5 long	b	0 - 5 m	± 0.01 m	5	(2)

Recording system:

a) Pressure transducer connected with datalogger by digital system.

b) Pressure transducer connected with datalogger by analogue system.

c) Manual recording.

d) Acoustic Doppler flow meter with on-board recording system.

Notes:

1) Expected uncertainty obtained from the WinFlume software. The lowest error corresponds to the highest discharge.

2) Overall expected uncertainty considering the characteristics of the water level sensor, the installation setup, the calibration method and the GPS error.

3) Measurement range is theoretical considering the dimension of the control section as a limiting factor. Expected uncertainty considers that the sensor accuracy is less than 1% of the measured values (flow velocity).

2.3 Water balance computation

For each of the study sites, a seasonal water balance was set up as shown in Eq. 1, considering a time period spanning from the first to the last day of the flooding period both in the summer and

winter seasons. A field control volume ranging from the top of the ponding water to the bottom of the rice root zone was considered:

$$\Delta S = R + Q_{IN} - Q_{OUT} - ET_C - SP \quad \text{(Eq. 1)}$$

where ΔS includes both the variation in the ponding water (ΔL) and in the soil moisture ($\Delta\theta$) within the rice root zone, R is the total rainfall, Q_{IN} is the irrigation inflow, Q_{OUT} is the irrigation outflow, ET_C is the evapotranspiration from soil and/or ponding water and the rice crop, and, finally, SP is a term which includes two main processes: net percolation, namely the net vertical flux at the bottom of the root zone volume (directed downward in flooding conditions), and the net lateral seepage (Bouman et al., 2007; Facchi et al., 2018). In the three pilot areas, since the groundwater level is rather shallow, becoming very shallow (< 1 m) during the flooding periods, the net lateral seepage was assumed to reduce to that through the paddy field bunds.

All the terms in Eq. 1 are used to solve the residual term of the water balance, SP, as seen in Eq. 2. ΔS is assumed to be null in the seasonal balance; this is explained by the fact that ΔL is assumed to be zero, as the calculation period for the three pilot areas begins and ends just before and after the flooding of rice paddies. Since in previous studies conducted on paddy fields in northern Italy it was demonstrated that the variation of soil moisture $\Delta\theta$, from the beginning to the end of the cropping season within the soil control volume defined by the rice rooting depth is negligible with respect to the others terms of the seasonal water budget (e.g., ΔS was shown to represent about 0.1% of the total water budget for continuously flooded rice in Cesari de Maria et al., 2017), this term was considered negligible also in this study. All the terms in the Eq. 1 and Eq. 2 are expressed in mm; in the case of the irrigation inflow and outflow over the season (Q_{IN} and Q_{OUT}), water volumes were divided by the respective flooded areas.

$$SP = R + Q_{IN} - Q_{OUT} - ET_C \quad \text{(Eq. 2)}$$

Amongst the variables considered in the water budget, R, Q_{IN} and Q_{OUT} were measured at hourly time steps by means of the instrumentation described in the previous section. Conversely, ET_C was

calculated at the same time step by applying the single coefficient FAO-56 method (Eq. 3; Allen et al., 1998) based on the FAO modified Penman-Monteith equation.

$$ET_C = K_C \bullet ETo \quad \text{(Eq. 3)}$$

The reference evapotranspiration (*ETo*) was computed from hourly meteorological data measured at the Castello D'Agogna meteorological station. The time-varying crop coefficient (K_C) was assumed equal to 1.05 during winter time (K_C of free water bodies; Allen et al., 1998), while during summertime its value was defined according to the results of a previous study conducted nearby the pilot study areas, in which the value of a dry seeded rice was found to be: $Kc_{ini} = 0.35$, $Kc_{mid} = 1.1$, $Kc_{end} = 0.6$ (Mayer et al., 2019). Rice growth stages (*ini, dev, mid, end*; Allen et al. 1998) were registered by the farmer in the farm diary (site E) or obtained through the processing of ESA-Sentinel2 data (site Z; Facchi et al., 2020). When fields were flooded, the maximum value between rice *Kc* and water *Kc* (1.05) was considered in Eq. 3, while rice *Kc* was taken into account during drying periods. Due to the low perimeter-to-area ratio of the pilot sites Z and C, and because bunds surrounding the two areas are permanent, about three meters large at the seedbed level and often flanked by farm roads, lateral seepage can be considered a negligible term in *SP* (Eq. 2). In site E, the experimental platform consisted of six plots separated by bunds taking water from an irrigation channel located on the eastern side of the platform and delivering irrigation tail-water to a drainage channel on the western side of the platform (Figure 1, Box E). The bunds separating the experimental plots had a thickness at the seedbed of about one meter and, even if carefully built at the beginning of the experiment, they certainly allowed water exchanges among plots, especially during winter flooding, when the three flooded plots were surrounded by dry ones. However, lateral seepage was collected by drainage ditches (20-25 cm deep with respect to the seeding bed) built at both sides of the bunds, which reached the drainage channel at the foot of the six parcels (Figure 1, box E, western side) where the measurements of the total outflow from the whole platform were taken. For this reason, although in the case of the E site the lateral seepage through bunds was probably not negligible, the

term *SP* was representative only of the vertical percolation component, *P* for E site as well (i.e. lateral seepage was added to the total outflow and therefore included in the Q_{OUT} value).

2.4 Uncertainty calculations

Since *SP* is calculated as the residual term of the volumetric water balance, it was decided to evaluate its uncertainty based on error propagation of the other measured or estimated input or output terms. In particular, the uncertainty of *SP* (mm in the season) was calculated as the square root of the sum of squares of the uncertainties associated to each water balance component (Eq. 2), as proposed in Kennedy (2015):

$$W_{SP} = \sqrt{W_R^2 + W_{QIN}^2 + W_{QOUT}^2 + W_{ETC}^2} \quad \text{(Eq. 4)}$$

where W represents the uncertainty of the variables specified in the water balance equation (Eq. 2). Notably, values for W_{QIN} and W_{QOUT} were based on the expected measurement error shown in Table 2, and it was decided to consider the highest expected error (10%). The error for W_{ETC} was based on the error propagation of each instrument measuring the physical variables considered for computing ETo and K_C . The errors associated with each component are as follows: temperature (± 0.05 °C, as reported for instance by Thermometer by Apogee Instruments Inc.), relative humidity (± 1.8%, Hygrometer by PCE instruments), radiation (30 W m^{-2}, NR-Lite Net radiometer by Campbell) and wind speed (± 0.05 m s^{-1}, i.e. Ultrasonic anemometer Young 81000). The errors were then propagated along the time series of temperature, relative humidity, radiation and wind speed relative to the considered period (October 2017 – March 2019) to obtain the % error of each variable. Finally, errors were summed in order to obtain the ETo error, equal to 8.9%, which was used in the uncertainty calculations. Lastly, the error associated with precipitation, W_R, was considered equal to 5% in accordance to what reported in Kennedy (2015), given the absence of information related to the specific rain gauge installed at Castello D'Agogna.

3. Results and discussion

3.1 Groundwater table response to flooding

Groundwater levels inside and outside the flooding areas were monitored continuously for 18 months (October 2017- March 2019) for sites E, C and Z. Figure 2 shows the groundwater levels (m a.s.l.) registered at all the monitoring wells, allowing to compare trends and absolute values among sites, also by extrapolating the piezometric gradients at each site. Groundwater levels were computed by subtracting groundwater table depth monitored at each site from the topographic elevation, determined during the topographic survey. Figure 3 illustrates the groundwater table depth below the soil surface (cm) only for the monitoring wells inside the three flooded areas, which is a fundamental variable from the point of view of vertical percolation. The percolation is in fact not dependent on the position of the groundwater surface in m a.s.l. itself, but on its depth with respect to the topographic surface, and particularly with respect to the less conductive soil layer LCL (see Facchi et al., 2018, for more explanations on the dynamic of percolation fluxes in paddy fields). Rainfall data registered during the overall monitoring period are shown in the upper panel of both figures. With respect to site E, the shown data series are not those measured, but they were obtained for each parcel within the pilot site by averaging the nearest monitored data series, weighted by their distance to the main axis of the parcel; in particular, p1 to p6 indicate parcels from south to north in Figure 1 - Box E, and winter flooded parcels are followed by 'WF' to differentiate them from the non-winter flooded parcels. For all pilot sites, thick lines illustrate the groundwater behaviour for areas flooded during wintertime, while thin lines refer to dry areas in winter.

Figure 2 shows that during both winters the groundwater levels reached similar (or at least comparable) levels to those observed in summertime, when a larger portion of paddies is submerged in the surrounding territory. This is true for sites Z and C (Figure 2- Panels 2 and 3), denoting a good effectiveness of winter percolation in recharging the phreatic aquifer even with flooded areas

rather limited in extent (i.e., 36 and 85 ha are the surfaces of the two pilot areas). This does not apply for the pilot site E, due to the really small surfaces flooded in wintertime; however, slight differences among flooded (thick lines) and not flooded (thin lines) parcels can be observed also at this site (Figure 2 – Panel 4). Groundwater levels were slightly lower in the second winter than in the first one in all three areas. Figure 2 - Panel 2 shows that one out of three wells located outside the winter flooded area of site Z clearly responded both to summer and winter flooding periods. This could be due to its position with respect to the main groundwater flow direction (Z5; Figure 1 – Box C). On the contrary, piezometers Z3 and Z4 showed a weak response to flooding events during the first and the second winters. In the case of site C, piezometers C2 and C1 (Figure 1 – Box D) responded to winter flooding during both years, the first one probably for its position downstream of the study area, the second one because it was most likely downstream of another flooded area during wintertime. Conversely, C4 seemed to respond the least to winter flooding. Figure 3 shows clearly that the time needed for groundwater to return to pre-flooding levels was overall faster after the winter flooding (about one month) than after the summer flooding (from two to two and a half months) in all three areas (Figure 3 – Panels 2 to 4). This can be explained by the fact that during winter the three pilot areas are mainly surrounded by dry land (only 3-4% of rice areas in Lombardy and Piedmont implemented this practice), whereas in summertime they are surrounded by flooded paddies providing recharge to groundwater for many tens of square kilometres upstream from the study areas. Moreover, the dates of cessation of summer flooding varies in space, while winter flooding ceases in all farms at the same time, on the day when the irrigation authority stops the irrigation service. Winter flooding as currently applied in northern Italy (areas very limited in extension and fragmented, end of the flooding on January 15th), has no effect on the groundwater levels at the beginning of the summer, which return to the pre-existing values before the agricultural season.

Moreover, Figure 3 highlights the fact that, even though the groundwater levels (m a.s.l.) can be different inside the pilot areas (Figure 2), the differences in terms of groundwater depths below the

topographical surface are much more limited, and practically null in summertime (i.e. the topographical gradient is very similar to the phreatic gradient, as shown in Figure 4 – Panel 3). Finally, Figure 3 shows that in the three sites the groundwater level reaches a maximum of about -40/50 cm from the soil surface.

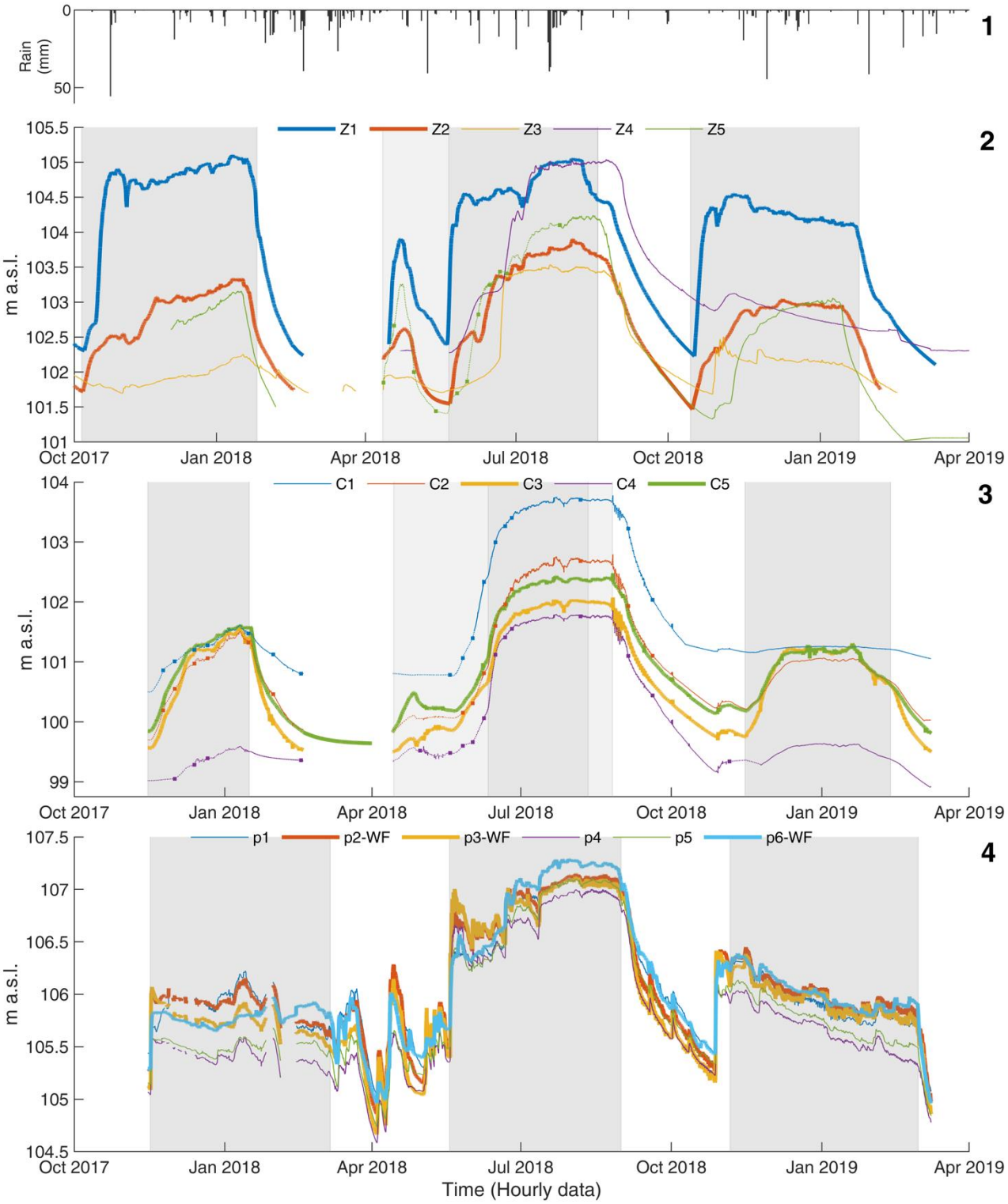

331

332 *Figure 2*

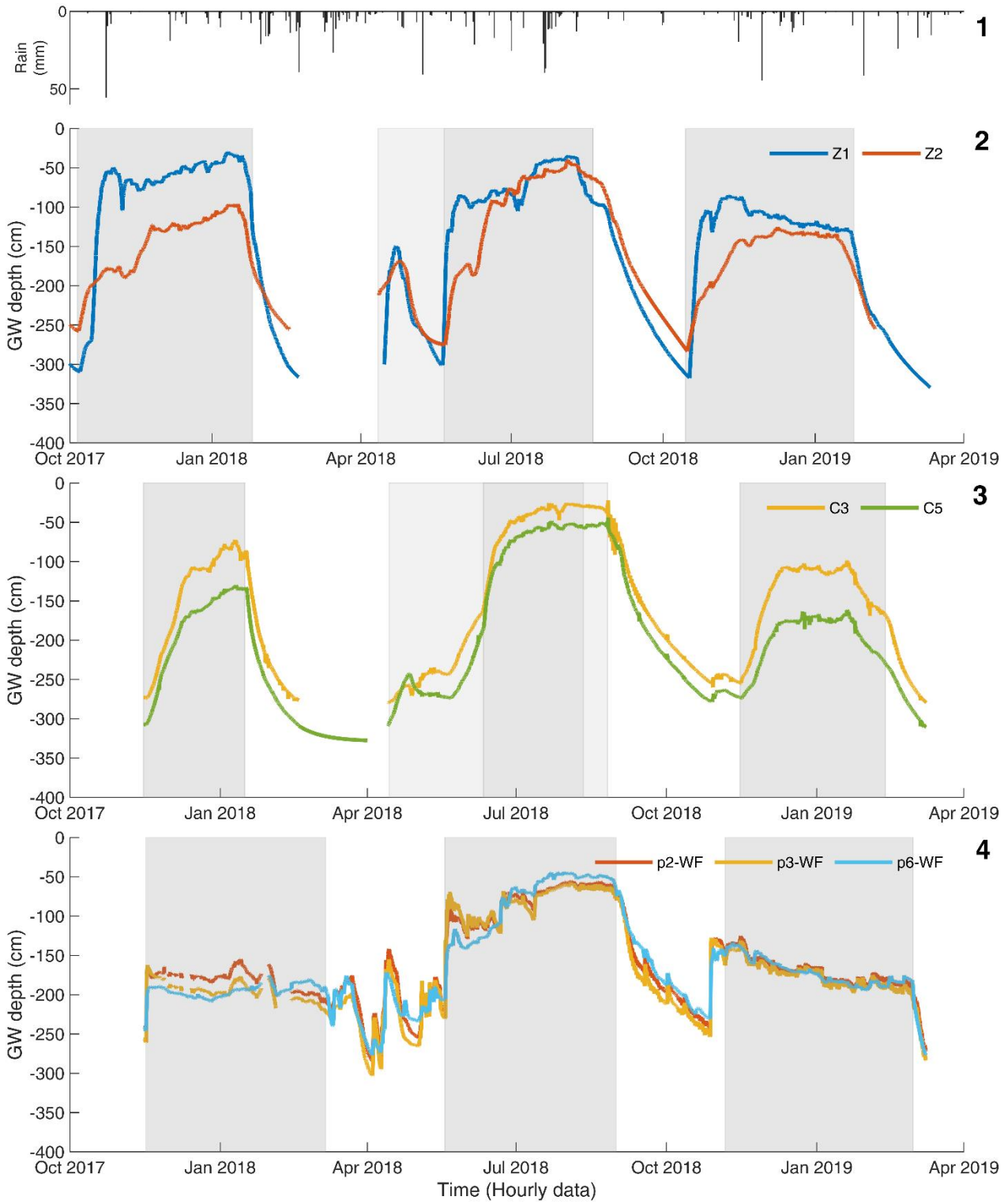

333

334 *Figure 3*

335 All that has been illustrated above regarding the effects of flooding periods on groundwater levels

336 can be summarized by Figure 4. In the literature, many studies are carried out in very small plots (a

337 few tens of square meters, such as site E, or even smaller), where percolation has a limited effect on

the observed aquifer level. The effect of the percolation flux on the groundwater level is stronger in the case of larger flooded areas (e.g. Z or C sites). However, as long as the recharge phenomenon remains local and it is not generated over very extended surface areas, the rise of the phreatic groundwater level is local (dark blue groundwater volumes in Figure 4 - Panels 1 and 2). As a consequence, groundwater piezometric gradients generated at the sides of the saturated soil volume are very high. Considering also the coarse nature of substrates in most of the investigated areas (high soil hydraulic conductivities), such gradients lead to important water fluxes that quickly deplete the water volume stored in the aquifer, producing a net water transfer downstream following the main flow direction of the regional aquifer (white arrows in Figure 4 – Panels 1 and 2). A different situation is that of the summer flooding (Figure 4 – Panel 3), where the recharge is widespread, and therefore the level of the regional aquifer rises simultaneously maintaining essentially its previous piezometric gradient.

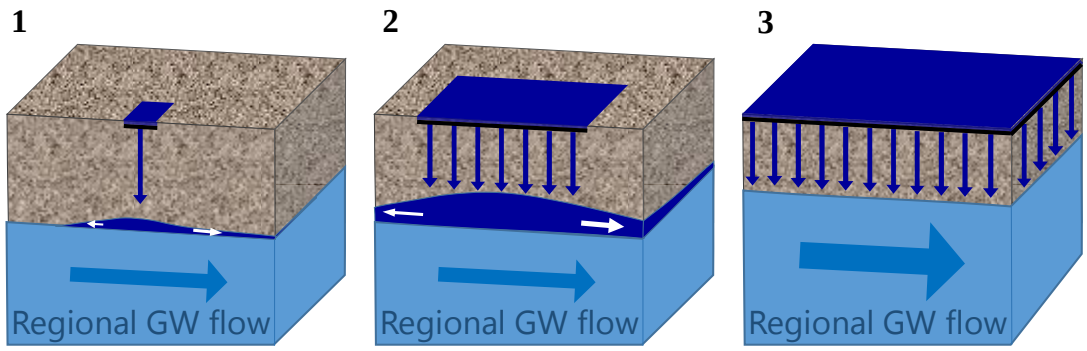

Figure 4

3.2 Soil water balance terms, percolation fluxes and uncertainty analysis

Results of the water balance for the three pilot areas are illustrated in Table 3, together with the results of the uncertainty analysis carried out for each water balance component (maximum computed uncertainty is shown with the ± symbol, similarly to a standard deviation). It should be noted that, both for winter and summer periods, ET_C values are referred to the flooded periods, hence, during summertime, ET_C is not referred to the whole cropping season, as flooding stops about 3 to 4 weeks before harvest and, in the case of dry-seeding, it starts about 3 weeks after the

359 sowing. However, ET_C for the whole cropping season is considered in the summer WUE calculation
360 (Table 3, sixth row). During floods, net water inflow (Q_{IN} - Q_{OUT}) accounted for about 90-99% of
361 water inputs, while precipitation accounted for 1.0-10%. With respect to the outputs, the residual
362 term (vertical percolation, P) accounted for 95.5-99.5% of the outputs in wintertime and 77.3-
363 84.5% in summertime (the remaining part being the ET_C term). WUE (Water Use Efficiency),
364 calculated with the approach proposed by Dunn and Gaydon (2011), was found to be 26.5% in the
365 Z site and 22.0% in site E during the summer of 2018. These values are consistent with the WUE
366 values measurements in other studies conducted in the Italian rice areas. In fact, Facchi et al.,
367 (2018) reported an average WUE value of 24.5% for a group of two productive rice fields (16 ha)
368 managed with dry seeding and delayed flooding. Cesari de Maria et al. (2017) found WUEs of 17
369 and 21% in experimental rice parcels managed with wet seeding-traditional flooding and dry
370 seeding-delayed flooding, respectively; in that study, the experimental platform was located in the
371 same farm as that in site E, and experimental plots were roughly the same size. Moreover, Mayer et
372 al., (2019) calculated average WUEs of 23% and 32% for traditionally flooded rice under shallow
373 and very deep groundwater conditions respectively, in a rice irrigation district of about 1000 ha
374 located in Lombardy (28% being the average WUE over the area). Very low winter WUEs are
375 obviously of no interest since the crop is absent and are reported in Table 3 for the sake of
376 comparison only.
377 To compare percolations between different sites and seasons, we introduced the variable “Average
378 percolation efficiency (%)” (Table 3), which is defined as the mathematical ratio between
379 Percolation and the sum of net inputs, Rainfall plus Surface Water Inflow minus Surface Water
380 Outflow. The efficiency of winter percolation is higher than that of summer, since on average 96%
381 of the water applied to the fields percolates below the rooting zone, compared to an average of 81%
382 observed in summer due to higher evapotranspiration fluxes. The daily percolation rates proved to
383 be very similar in each pilot area in the two winters, and vary between a value of 17 mm day^{-1} at
384 site E, where soils are finer (texture: loam/loam/silt loam–silty clay, in the soil horizons A/B/BC-C

385 respectively) and the irrigation management is more controlled (i.e. site E is an experimental
386 platform), and values of 40 and 48 mm day^{-1} for the Z and C sites (sandy loam/sandy loam-
387 loam/sandy loam-loam, in the soil horizons A/B/BC-C). It should be noted that in the Z site the
388 percolation rate in the two winters is slightly lower than in the C site, although soils are coarser in
389 some areas (textural classes are the same in the two pilot areas, but from the soil survey it emerged
390 that in the Z site the main soil type is crossed by 'strips' of a coarser soil). The summer percolation
391 rate (23 mm day^{-1}) is slightly higher than the winter one at site E, as expected considering the effect
392 of water temperature on water viscosity, and consequently on saturated soil hydraulic conductivity
393 (average temperatures of ponding water during winter and summer months are 6° and 25°C,
394 respectively). On the contrary, the percolation rate is much lower than in winter at the pilot site Z
395 (16 mm day^{-1}). This anomaly cannot be explained only by the lower ponding water level during
396 summer compared to winter (about 100 mm from the seedbed in summertime *vs* about 160 mm in
397 wintertime, values obtained from manual measurements made in some fields at site Z), and by a
398 higher groundwater level. The most plausible hypothesis to explain it is a change in the soil
399 hydraulic conductivity (in particular of the low conductive soil layer, LCL, as defined in Facchi et
400 al., 2018), probably due to the effect of a winter flooding practice conducted over a long period of
401 time (since 2004) on the soil permeability. Preliminary results of a hydrological modelling exercise,
402 carried out by applying a soil water balance approach based on a Darcy-type model (Facchi et al.,
403 2018), are presented in Facchi et al (2020) for the site Z. Anyway, the reason of this change in
404 hydraulic conductivity is unknown, but it could be due mainly to bio-clogging phenomena (increase
405 in bacterial biomass, as well as in extracellular polymeric substances - EPS - and gases produced by
406 bacteria at high temperatures; Seki et al., 1996). The change in saturated soil hydraulic conductivity
407 may not have occurred at site E (indeed, hydraulic conductivity increased in the expected way in
408 summer considering the effect of the increased in temperature on the viscosity of the water) because
409 this site has been adopting winter flooding for less time (2016) and it is an experimental site in
410 which soil tillage is applied punctually every year and winter and summer flooding covers periods

fairly limited in time. On the contrary, site Z is within a productive farm where tillage practices are not carried out every year, the use of agrochemicals is limited as much as possible, and winter flooding has been practiced for a long time and maintained for as long as possible (in one of the fields of the Z site, for instance, sowing in the summer of 2018 took place without draining the water from the winter flooding). These different management practices could explain the differences in summer percolation rates when compared to the respective winter ones, but deeper investigations (including microbiological ones) are essential to state something certain.

Table 3

	Z site			C site		E site		
Water balance components	**First winter**	**First summer**	**Second winter**	**First winter**	**Second winter**	**First winter**	**First summer**	**Second winter**
Rainfall (*R*, mm)	117.0 ± 5.8	260.0 ± 13.0	179.8 ± 9.0	40.0 ± 2.0	42.0 ± 2.1	85 ± 4.2	134.2 ± 6.7	63.8 ± 3.2
Net surface irrigation (Q_{IN}-Q_{OUT}, mm)	4181.6 ± 658.5	2388.0 ± 829.1	4141.4 ± 660.1	3196.4 ± 319.7	4247.1 ± 425.7	1700.6 ± 908.6	2834.8 ± 627.5	1958.0 ± 1046.1
Evapotranspiration (ET_C, mm)	52.6 ± 4.6	600.2 ± 53.3	67.2 ± 6.0	15.7 ± 1.4	51.1 ± 4.5	41.4 ± 3.6	466.3 ± 41.4	91.8 ± 8.2
WUE (%) [ET_C/(R+Q_{IN}-Q_{OUT})*100]	1.2	26.5	1.6	0.5	1.2	2.3	22.0	4.5
Residual term (P, mm)	4246.0 ± 669.9	2047.8 ± 868.9	4254.5 ± 682.5	3220.7 ± 321.1	4238.0 ± 425.7	1724.8 ± 222.0	2502.7 ± 1062.0	1930.0 ± 251.7
Average percolation rate (mm/day)	40.1	15.8	41.7	51.9	47.6	15.7	23.8	16.8
Average percolation efficiency (%) [P/(R+Q_{IN}-Q_{OUT})*100]	95.0	77.0	97.0	91.5	96.9	96.6	80.8	94.5
Average (and maximum 'plateau' value) water table depth (m)	1.2 (1.0)	1.3 (0.5)	1.5 (1.3)	1.7 (1.3)	1.7 (1.5)	1.9 (not present)	0.9 (0.6)	1.7 (not present)
Average texture (USDA)	SL/SL-L/SL-L			SL/SL-L/SL-L		L/L/SiL-SiC		

Winter percolation rates found in the three rice pilot study areas are in line with those presented in other water balance studies. In particular, Dokoozlian et al., (1987) calculated an average percolation rate of 80 mm day^{-1} during the winter flooding of grapevines on a clay-loam soil in 1981-1985 in the San Joaquin Valley, California; ponding water was maintained at 150 mm above the soil surface. Bachand et al. (2016, 2014) reported percolation rates between 68 and 400 mm day^{-}

426 [1] during flooding events carried out on 405 ha of croplands within the Kings River Basin,
427 California; ponding water level was kept between 150 and 300 mm. In these studies, soils were
428 reported to be mostly fine sandy loam, loam coarse sands and loamy sands, and groundwater table
429 levels were deep (18-24 m below the surface). Kennedy (2015) reported lower percolation rates for
430 winter flooding of cranberry fields in south-eastern Massachusetts, with values spanning between
431 12 and 15 mm day^{-1}; the study area was characterized by coarse-medium sands.
432

433 ## 4. Conclusions

434 This paper presents the results of an intensive hydrological monitoring campaign focused on
435 investigating the effects of winter flooding on the hydrological balance of rice areas in northern
436 Italy and carried out in three pilot rice areas during 18 months (winter seasons 2017-2018 and 2018-
437 2019, and summer season 2018). Such a study was deemed of wide interest, as data on this issue are
438 scarcely available worldwide, with none available for Italy.
439 Results illustrate that during the summer season, the pilot areas showed a hydrological balance
440 similar to that reported in other studies conducted in the same geographical area (WUE between 20
441 and 30%). Winter percolation rates were found to be very similar for each site in the two winters,
442 but different from site to site, denoting a high site-specificity, mainly connected to soil properties.
443 During the winter flooding, a lower percolation rate compared to that in summer was observed for
444 one of the pilot sites, located within an experimental platform where the winter flooding practice
445 has been adopted only recently (since 2016). The increased summer percolation rate can be justified
446 by the lower water viscosity (leading to a higher soil hydraulic conductivity) due to the higher
447 summer temperatures. Conversely, percolation reduced by more than half compared to winter was
448 observed in the other pilot site in which the hydrological balance was investigated both in summer
449 and winter. The low summer percolation rate in this second pilot site could be justified only
450 partially by the lower ponding water level maintained over the fields, and by the higher
451 groundwater levels reached during the summer season. To explain it, a change in paddy soil

hydraulic conductivity shall be assumed, and this may be connected to an increase in the soil microbial activity at summer temperatures in this second pilot area. This could lead to say that the summer WUE could be increased by the winter flooding in paddies characterized by a high degree of naturalness and under prolonged flooding conditions within year and over the years. However, further investigations must be conducted before anything certain can be stated to explain the observed phenomenon.

With respect to the effects on groundwater resources, during the winter flooding, groundwater levels reached nearly the same value than during the cropping season, when flooding is applied over larger areas. However, when winter flooding stopped, the groundwater depletion rate was faster (about one month to return to pre-winter flooding levels) compared to the depletion rate following the summer flooding (from two to two and a half months). This is mainly due to the fact that winter flooded areas are surrounded by dry land (only 3-4% of the rice areas implemented the practice in the whole Lombardy-Piedmont rice basin), while a large surface upstream of the study sites along the main groundwater flow direction is flooded during the cropping season. Consequently, to maintain the phreatic aquifer at higher levels at the beginning of the summer (which would reduce water percolation losses from the agricultural fields and within the irrigation network, thus increasing the WUE of rice agro-ecosystems during the cropping season), winter flooding should be ended not long before the summer flooding, and should be adopted over larger and more contiguous areas.

Modelling applications to the collected dataset, aimed at better interpreting the experimental measurements and generalize the results, are beyond the scope of this study and will be the subject of a next article.

Acknowledgements: We wish to thank Regione Lombardia for funding the RISTEC project (EU-RDP 2017), in the context of which this research was developed.

Research data for this article

The datasets generated during the current study are available from the corresponding author on reasonable request.

Bibliography

Allen, R.G., Pereira, L.S., Raes, D., Smith, M., 1998. FAO Irrigation and drainage paper No. 56. Rome Food Agric. Organ. U. N. 26–40.

Anders, M.M., van Kessel, K., Eadie, J.M., 2008. Agronomic impacts of winter wetland and waterfowl management in Ricelands. Conserv. Ricelands N. Am. 91–117.

Bachand, P.A.M., Roy, S.B., Choperena, J., Cameron, D., Horwath, W.R., 2014. Implications of Using On-Farm Flood Flow Capture To Recharge Groundwater and Mitigate Flood Risks Along the Kings River, CA. Environ. Sci. Technol. 48, 13601–13609. https://doi.org/10.1021/es501115c

Bachand, P.A.M., Roy, S.B., Stern, N., Choperena, J., Cameron, D., Horwath, W.R., 2016. On-farm flood capture could reduce groundwater overdraft in Kings River Basin. Calif. Agric. 70, 200–207. https://doi.org/10.3733/ca.2016a0018

Bouman, B.A.M., Lampayan, R.M., Tuong, T.P., 2007. Water Management in Irrigated Rice: Coping with Water Scarcity. Int. Rice Res. Inst., Los Baños.

Brogi, A., Pernollet, C.A., Gauthier-Clerc, M., Guillemain, M., 2015. Waterfowl foraging in winter-flooded ricefields: Any agronomic benefits for farmers? Ambio 44, 793–802. https://doi.org/10.1007/s13280-015-0678-0

Cesari de Maria, S., Bischetti, G.B., Chiaradia, E.A., Facchi, A., Miniotti, E.F., Rienzner, M., Romani, M., Tenni, D., Gandolfi, C., 2017. The role of water management and environmental factors on field irrigation requirements and water productivity of rice. Irrig. Sci. 35, 11–26. https://doi.org/10.1007/s00271-016-0519-3

Chen, S.-K., Liu, C.W., Huang, H.-C., 2002. Analysis of water movement in paddy rice fields (II) simulation studies. J. Hydrol. 268, 259–271. https://doi.org/10.1016/S0022-1694(02)00180-4

Chiaradia, E.A., Facchi, A., Masseroni, D., Ferrari, D., Bischetti, G.B., Gharsallah, O., Cesari de Maria, S., Rienzner, M., Naldi, E., Romani, M., Gandolfi, C., 2015. An integrated, multisensor system for the continuous monitoring of water dynamics in rice fields under different irrigation regimes. Environ. Monit. Assess. 187, 586. https://doi.org/10.1007/s10661-015-4796-8

508 Dahlke, H.E., Brown, A.G., Orloff, S., Putnam, D., O'Geen, T., 2018. Managed winter flooding of
509 alfalfa recharges groundwater with minimal crop damage. Calif. Agric. 72, 1–11.
510 https://doi.org/10.3733/ca.2018a0001
511 Dokoozlian, N.K., Petrucci, V.E., Ayars, J.E., Clary, C.D., Schoneman, R.A., 1987. Artificial
512 Ground Water Recharge by Flooding During Grapevine Dormancy1. JAWRA J. Am. Water
513 Resour. Assoc. 23, 307–311. https://doi.org/10.1111/j.1752-1688.1987.tb00809.x
514 Dunn, B.W., Gaydon, D.S., 2011. Rice growth, yield and water productivity responses to irrigation
515 scheduling prior to the delayed application of continuous flooding in south-east Australia. Agric.
516 Water Manag. 98, 1799–1807. https://doi.org/10.1016/j.agwat.2011.07.004
517 Facchi, A., Negri, C., Rienzner, M., Chiaradia, E., Romani, M., 2020. Groundwater Recharge
518 Through Winter Flooding of Rice Areas, in: Coppola, A., Di Renzo, G.C., Altieri, G., D'Antonio,
519 P. (Eds.), Innovative Biosystems Engineering for Sustainable Agriculture, Forestry and Food
520 Production, Lecture Notes in Civil Engineering. Springer International Publishing, Cham, pp. 79–
521 87. https://doi.org/10.1007/978-3-030-39299-4_9
522 Facchi, A., Rienzner, M., Cesari de Maria, S., Mayer, A., Chiaradia, E.A., Masseroni, D., Silvestri,
523 S., Romani, M., 2018. Exploring scale-effects on water balance components and water use
524 efficiency of toposequence rice fields in Northern Italy. Hydrol. Res. 49, 1711–1723.
525 https://doi.org/10.2166/nh.2018.125
526 Fogliatto, S., Vidotto, F., Ferrero, A., 2010. Effects of winter flooding on weedy rice (Oryza sativa
527 L.). Crop Prot. 29, 1232–1240. https://doi.org/10.1016/j.cropro.2010.07.007
528 Kaneko, K., Nakamura, T., 2011. Effects of the inhibition of weed communities by winter-flooding.
529 Agric. Sci. 02, 383–391. https://doi.org/10.4236/as.2011.24050
530 Kennedy, C.D., 2015. Hydrologic and nutrient response of groundwater to flooding of cranberry
531 farms in southeastern Massachusetts, USA. J. Hydrol. 525, 441–449.
532 https://doi.org/10.1016/j.jhydrol.2015.02.038
533 Koger, C.H., Zablotowicz, R.M., Weaver, M.A., Tucker-Patterson, M.R., Krutz, J.L., Walker, T.W.,

534 Street, J.E., 2013. Effect of Winter Flooding on Weeds, Soybean Yield, Straw Degradation, and
535 Soil Chemical and Biochemical Characteristics. Am. J. Plant Sci. 04, 10–18.
536 https://doi.org/10.4236/ajps.2013.47A2002
537 Lin, H.-C.J., Richards, D.R., Yeh, G.-T., Cheng, J.-R., Cheng, H.-P., 1997. FEMWATER: A Three-
538 Dimensional Finite Element Computer Model for Simulating Density-Dependent Flow and
539 Transport in Variably Saturated Media. (No. WES/TR/CHL-97-12). ARMY ENGINEER
540 WATERWAYS EXPERIMENT STATION VICKSBURG MS COASTAL HYDRAULICS LA B.
541 Manley, S.W., 1999. Ecological and agricultural values of winter-flooded ricefields in Mississippi.
542 Ph.D. Dissertation.
543 Mayer, A., Rienzner, M., Cesari de Maria, S., Romani, M., Lasagna, A., Facchi, A., 2019. A
544 Comprehensive Modelling Approach to Assess Water Use Efficiencies of Different Irrigation
545 Management Options in Rice Irrigation Districts of Northern Italy. Water 11, 1833.
546 https://doi.org/10.3390/w11091833
547 Miller, M.R., Garr, J.D., Coates, P.S., 2010. Changes in the Status of Harvested Rice Fields in the
548 Sacramento Valley, California: Implications for Wintering Waterfowl. Wetlands 30, 939–947.
549 https://doi.org/10.1007/s13157-010-0090-2
550 Natuhara, Y., 2013. Ecosystem services by paddy fields as substitutes of natural wetlands in Japan.
551 Ecol. Eng., Bringing Together Science and Policy to Protect and Enhance Wetland Ecosystem
552 Services in Agricultur 56, 97–106. https://doi.org/10.1016/j.ecoleng.2012.04.026
553 Niang, A., Pernollet, C.A., Gauthier-Clerc, M., Guillemain, M., 2016. A cost-benefit analysis of
554 rice field winter flooding for conservation purposes in Camargue, Southern France. Agric. Ecosyst.
555 Environ. 231, 193–205. https://doi.org/10.1016/j.agee.2016.06.018
556 Niswonger, R.G., Morway, E.D., Triana, E., Huntington, J.L., 2017. Managed aquifer recharge
557 through off-season irrigation in agricultural regions: MANAGED AQUIFER RECHARGE IN
558 AGRICULTURE. Water Resour. Res. 53, 6970–6992. https://doi.org/10.1002/2017WR020458
559 Pernollet, C.A., Guelmami, A., Green, A.J., Curcó Masip, A., Dies, B., Bogliani, G., Tesio, F.,

560 Brogi, A., Gauthier-Clerc, M., Guillemain, M., 2015. A comparison of wintering duck numbers
561 among European rice production areas with contrasting flooding regimes. Biol. Conserv. 186, 214–
562 224. https://doi.org/10.1016/j.biocon.2015.03.019
563 Serra, P., More, G., Pons, X., 2007. Monitoring winter flooding of rice fields on the coastal wetland
564 of Ebre delta with multitemporal remote sensing images, in: 2007 IEEE International Geoscience
565 and Remote Sensing Symposium. Presented at the 2007 IEEE International Geoscience and Remote
566 Sensing Symposium, IEEE, Barcelona, Spain, pp. 2495–2498.
567 https://doi.org/10.1109/IGARSS.2007.4423350
568 Taghavi, A., Blanke, J., Cayar, M., 2015. A New Opportunity: Groundwater Recharge through
569 Winter Flooding of Agricultural Land in the San Joaquin Valley.
570 Wopereis, M.C.S., Bouman, B.A.M., Kropff, M.J., ten Berge, H.F.M., Maligaya, A.R., 1994. Water
571 use efficiency of flooded rice fields I. Validation of the soil-water balance model SAWAH. Agric.
572 Water Manag. 26, 277–289. https://doi.org/10.1016/0378-3774(94)90014-0
573